PNAS RESEARCH ARTICLE | NEUROSCIENCE

Seizure-induced strengthening of a recurrent excitatory circuit in the dentate gyrus is proconvulsant

Kaoutsar Nasrallah[a,1], M. Agustina Frechou[a,b], Young J. Yoon[a,c], Subrina Persaud[a], J. Tiago Gonçalves[a,b], and Pablo E. Castillo[a,d,1]

Edited by Thomas Südhof, Stanford University, Stanford, CA; received January 20, 2022; accepted June 27, 2022

Epilepsy is a devastating brain disorder for which effective treatments are very limited. There is growing interest in early intervention, which requires a better mechanistic understanding of the early stages of this disorder. While diverse brain insults can lead to epileptic activity, a common cellular mechanism relies on uncontrolled recurrent excitatory activity. In the dentate gyrus, excitatory mossy cells (MCs) project extensively onto granule cells (GCs) throughout the hippocampus, thus establishing a recurrent MC-GC-MC excitatory loop. MCs are implicated in temporal lobe epilepsy, a common form of epilepsy, but their role during initial seizures (i.e., before the characteristic MC loss that occurs in late stages) is unclear. Here, we show that initial seizures acutely induced with an intraperitoneal kainic acid (KA) injection in adult mice, a well-established model that leads to experimental epilepsy, not only increased MC and GC activity in vivo but also triggered a brain-derived neurotrophic factor (BDNF)–dependent long-term potentiation (LTP) at MC-GC excitatory synapses. Moreover, in vivo induction of MC-GC LTP using MC-selective optogenetic stimulation worsened KA-induced seizures. Conversely, *Bdnf* genetic removal from GCs, which abolishes LTP, and selective MC silencing were both anticonvulsant. Thus, initial seizures are associated with MC-GC synaptic strengthening, which may promote later epileptic activity. Our findings reveal a potential mechanism of epileptogenesis that may help in developing therapeutic strategies for early intervention.

hippocampus | mossy cell | epilepsy | granule cell | BDNF

Significance

Better understanding of the initial molecular and cellular processes implicated in epileptogenesis is essential for early therapeutic intervention (i.e., before brain damage becomes irreversible). Uncontrolled activity of recurrent excitatory circuits is a common mechanism that promotes epileptic activity. In the dentate gyrus, mossy and granule cells form a recurrent excitatory circuit that can be strengthened upon activity and whose dysregulation has been implicated in temporal lobe epilepsy. Here, we found that acute induction of seizures triggers robust brain-derived neurotrophic factor (BDNF)–dependent strengthening of mossy cell–granule cell synapses that promotes further convulsive seizures. Moreover, blocking this synaptic strengthening prevents seizure activity. Together, our findings provide a potential mechanism for early epileptogenesis involving BDNF within a recurrent hippocampal excitatory network.

Epilepsy is a common neurological disorder characterized by recurrent epileptic seizures, often associated with profound cognitive, psychological, and social deleterious consequences (1). About 30% of patients are resistant to antiseizure drugs (2). To develop more effective treatments, a better understanding of the cellular and molecular processes implicated in the early stages of epilepsy, before brain damage becomes irreversible, is required. Mossy cells (MCs), excitatory neurons in the dentate gyrus (DG) of the hippocampus, play a critical role in temporal lobe epilepsy (TLE) (3–5), the most common form of focal epilepsy in adults (6). However, whether MC activity can be pro- or antiepileptic has been a subject of debate for several decades (3–5, 7, 8). MC loss is a hallmark feature of chronic TLE in both human and animal models (9–13). Recent studies reported that while surviving MCs in a mouse model of chronic TLE play an antiepileptic role (4), these cells could be proepileptic early during initial experimental seizures (5, 14).

Aberrant recurrent excitatory activity is a core mechanism in epilepsy (15). In the DG, glutamatergic MCs and granule cells (GCs) are reciprocally connected, thus forming an intrinsic excitatory loop. Remarkably, a single MC makes more than 30,000 synaptic contacts onto GCs, locally, contralaterally, and along the longitudinal axis of the hippocampus (16, 17). Furthermore, repetitive stimulation of MC axons in vitro induces robust long-term potentiation (LTP) at MC-GC excitatory synapses (MC-GC LTP). The DG is characterized by very sparse GC activity (18–20), and it is believed to act as a gate that opens during epileptic seizures (21, 22). The long-lasting strengthening of MC-GC synaptic transmission is sufficient to overcome the basal strong GC inhibition, thereby allowing MCs to drive GCs and presumably open the DG gate (23). MC-GC LTP is mediated by brain-derived neurotrophic factor (BDNF)/tropomyosin receptor kinase B (TrkB) signaling (23, 24), which is known to promote TLE (25). Therefore, activity-dependent strengthening of MC-GC synapses may promote epilepsy through the extensive MC projections onto GCs. While an episode of prolonged seizures (e.g., status epilepticus) can result in TLE (26–28), it is unknown whether and how initial seizures can impact MC-GC synaptic strength.

Using multiple complementary approaches, such as chemogenetics, in vitro electrophysiology, in vivo optogenetics, in vivo calcium imaging, and a conditional knockout (cKO) strategy, we found that initial seizures not only increased MC and GC activity in vivo but also triggered a BDNF-dependent strengthening of MC-GC synaptic

Author contributions: K.N., M.A.F., Y.J.Y., J.T.G., and P.E.C. designed research; K.N., M.A.F., Y.J.Y., and S.P. performed research; Y.J.Y. contributed new reagents/analytic tools; K.N., M.A.F., Y.J.Y., S.P., and J.T.G. analyzed data; and K.N. and P.E.C. wrote the paper.

The authors declare no competing interest.

This article is a PNAS Direct Submission.

[1]To whom correspondence may be addressed. Email: kaoutsar.n@gmail.com or pablo.castillo@einsteinmed.edu.

This article contains supporting information online at http://www.pnas.org/lookup/suppl/doi:10.1073/pnas.2201151119/-/DCSupplemental.

Published August 5, 2022.

transmission. In addition, in vivo induction of MC-GC LTP was sufficient to promote convulsive seizures, whereas interfering with BDNF signaling and MC activity had an anticonvulsant effect. Our findings support a proepileptic role of MCs and BDNF in epileptogenesis and provide a potential causal link between MC-GC LTP and epilepsy.

Results

Chemogenetic Silencing of MCs Reduced Acute Kainic Acid–Induced Seizures. To test the hypothesis that MC-GC LTP has a proconvulsant effect during early epilepsy, we first tested the prediction that silencing MCs should reduce the severity/susceptibility of experimental seizures induced by a single intraperitoneal (IP) injection of kainic acid (KA), a well-established experimental model that leads to later epilepsy (29, 30). A relatively high dose of KA (30 mg/kg) was used to induce strong seizures, which facilitates the detection of a potential decrease in seizure susceptibility/severity. To suppress MC output, the G_i inhibitory designer receptor exclusively activated by a designer drug [hM4D(G_i) or iDREADD] was selectively expressed in MCs. We bilaterally injected a Cre-recombinase–dependent virus expressing the iDREADD under the CaMKII promoter [adeno-associated virus (AAV)-CaMKII-DIO-hM4D(G_i)-mCherry] into the DG of *Drd2*-Cre mice, whereas *Drd2*-Cre mice injected with AAV-CaMKII-DIO-mCherry served as control (Fig. 1*A*). Consistent

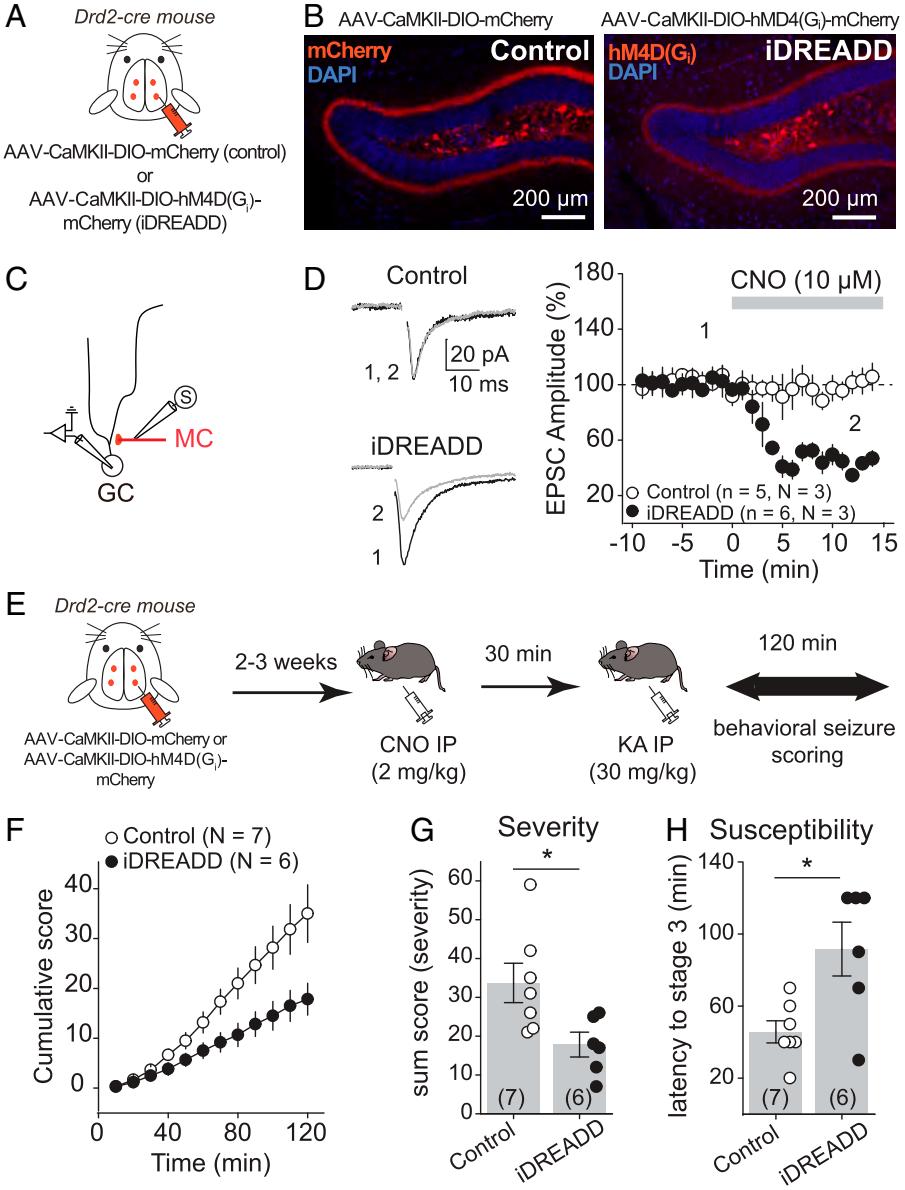

Fig. 1. Chemogenetic silencing of MCs reduced acute KA-induced seizures. (*A* and *B*) AAV expressing mCherry (control, AAV-CaMKII-DIO-mCherry) or the iDREADD hM4D(G_i)-mCherry [AAV-CaMKII-DIO-hM4D(G_i)-mCherry] were bilaterally injected into the ventral and dorsal DG of *Drd2*-cre mice. Confocal images of the DG show how the viral expression is selective for hilar MCs. Note the dense labeling of MC axons in the IML. (*C*) Schematic diagram illustrating the recording configuration. Evoked MC EPSCs were recorded from GC in response to MC axon stimulation in the IML. (*D*) Representative traces (*Left*) and time course plot (*Right*) showing that CNO significantly reduced EPSC amplitude in slices expressing iDREADD in MCs but not in controls. Here and in all figures, *n* indicates the number of cells and *N* indicates the number of animals. (*E*) Experimental timeline. Viral stereotaxic injections were performed in *Drd2*-cre mice to express control (AAV-CaMKII-DIO-mCherry) or iDREADD in MCs [AAV-CaMKII-DIO-hM4D(G_i)-mCherry] 2 to 3 wk before assessing behavioral seizures (for 120 min). All animals were treated with CNO in vivo (2 mg/kg, IP) 30 min before seizures were acutely induced with a single KA IP injection (30 mg/kg). (*F–H*) Chemogenetic silencing of MCs reduced seizure severity and susceptibility. Scoring of seizures using a modified Racine scale for 120 min revealed significant decreases in the cumulative seizure score (*F*) and in the sum score (*G*) and a significantly increase in latency to convulsive seizures (*H*) when MCs were silenced as compared with control animals. Each number in parentheses indicates the number of animals. *$P < 0.5$. Data are presented as mean ± SEM. Here and in all figures, error bars indicate SEM.

with previous reports (5, 31), we found that the viral expression was selective to MCs (Fig. 1*B*). Next, we verified that iDREADD efficiently responded to the DREADD agonist clozapine *N*-oxide (CNO). Bath application of 10 μM CNO strongly inhibited MC activity in iDREADD-expressing cells (*SI Appendix*, Fig. S1) and significantly reduced the amplitude of evoked MC-GC excitatory postsynaptic currents (EPSCs) in acute slices obtained from *Drd2*-Cre mice injected with AAV-CaMKII-DIO-hM4D(G_i)-mCherry but not with AAV-CaMKII-DIO-mCherry (Fig. 1 *C* and *D*) (iDREADD: 43.8 ± 4.3% of baseline, $n = 6$, $P = 0.0005$, paired *t* test; control: 100.6 ± 5.5% of baseline, $n = 5$, $P = 0.92$, paired *t* test). We then monitored and scored behavioral seizures induced by KA IP injection (30 mg/kg) for 2 h (see *Materials and Methods*) in both *Drd2*-Cre mice injected with AAV-CaMKII-DIO-hM4D(G_i)-mCherry (iDREADD) or AAV-CaMKII-DIO-mCherry (control). The two groups were injected with CNO (2 mg/kg, IP) 30 min before KA administration (30 mg/kg, IP) (Fig. 1*E*). Consistent with a recent study using the pilocarpine model (5), we found that silencing MCs reduced seizure severity and susceptibility, as indicated by significant decreases in the total cumulative seizure score (Fig. 1*F*) [two-way ANOVA repeated measure (RM); AAV condition: $F(1,5) = 7.2$, $P = 0.04$; time: $F(1.1,5.6) = 71.7$, $P = 0.0002$; AAV condition × time: $F(1,5) = 88.1$, $P = 0.002$] and in the sum score (Fig. 1*G*) [control: 33.7 ± 5.1, $n = 7$; iDREADD: 17.8 ± 3.2, $n = 6$; control vs. iDREADD: $P = 0.02$, unpaired *t* test] and an increase in latency to stage 3 (Fig. 1*H*) (control: 45.7 ± 6.1, $n = 7$; iDREADD: 91.7 ± 14.9, $n = 6$; control vs. iDREADD: $P = 0.01$, unpaired *t* test). These results reinforce the notion that MC activity has a proconvulsant effect during initial drug-induced seizures.

Initial Convulsive Seizures Potentiated MC-GC Transmission Presynaptically. We hypothesized that early seizures may increase MC activity and thus induce MC-GC LTP in vivo. MC repetitive activity is sufficient to trigger a robust MC-GC LTP in acute brain slices obtained from healthy rodents (23). Furthermore, a recent in vivo study using a calcium indicator and fiber photometry reported that DG neuronal activity is increased during KA-induced seizures (32). However, the contribution of specific subtypes of neurons, including MCs and GCs, remains unknown. We therefore monitored MC and GC activity in vivo using calcium imaging during acutely induced seizures. To this end, we expressed the genetically encoded Ca^{2+} indicator jRGECO1a selectively in DG excitatory neurons (*SI Appendix*, Fig. S2 *A–C*) by unilaterally injecting AAV-CaMKII-jRGECO1a into the DG of wild-type (WT) adult mice. The animals were then implanted with a chronic imaging window above the dorsal hippocampus, and MC and GC activity was visualized using head-fixed two-photon imaging before and during acute seizures (Fig. 2 *A* and *B*). After collecting basal activity, seizures were induced with a single KA IP injection (30 mg/kg). Neuronal activity was monitored during stage 3 of convulsive seizures, which was determined by the presence of forelimb clonus. Saline-injected mice served as a control. We found that during KA-induced convulsive seizures both MCs and GCs displayed robust calcium waves, which were absent from saline-injected mice (Fig. 2 *C–F*). In total, we recorded 117 MCs and 1,132 GCs from four saline-injected mice and 127 MCs and 1,162 GCs from five KA-injected mice (Fig. 2 and *SI Appendix*, Fig. S2 *D* and *E*). The convulsion-associated calcium waves were observed in almost all (~99%) recorded GCs and MCs and likely indicated strong, synchronized neural activity in GCs (Fig. 2*E*) (KA $\Delta F/F$ per cell = 2.226 ± 0.016, $P < 0.00001$, ANOVA; KA $\Delta F/F$ per mouse = 2.202 ± 0.181, $P = 0.0159$, Mann–Whitney *U* test) and MCs (Fig. 2*F*) (KA $\Delta F/F$ per cell = 1.756 ± 0.058, ANOVA; KA $\Delta F/F$ per mouse = 1.793 ± 0.071, $P = 0.0159$, Mann–Whitney *U* test). In addition, the seizure-associated calcium waves in GCs were significantly delayed compared with MCs, as indicated by a shift in changepoint (see *Materials and Methods*) (Fig. 2 *G–I*) ($GC_{changepoint} - MC_{changepoint}$ = 3.261 ± 1.170 s, $n = 5$ animals, $P = 0.049$, *t* test), suggesting that KA-induced MC activity precedes and may drive GCs.

We then tested whether initial KA-induced seizures, by increasing MC activity and inducing LTP, could strengthen MC-GC connections in vivo. We analyzed MC-GC synaptic transmission in both KA-injected and saline-injected mice. After a single KA injection (20 mg/kg, IP), the animals were monitored and killed humanely for acute hippocampal slice preparation once stage 3 of convulsive seizures was reached (Fig. 3*A*). Sham-injected mice were used as control. MC-GC synaptic function was assessed by activating MC axons while performing whole-cell voltage-clamp recordings from GCs. We found that MC-GC synaptic transmission was significantly strengthened, as indicated by an increase in the input/output function (Fig. 3*B*) [two-way ANOVA RM; IP injection: $F(1,9) = 6.5$, $P = 0.031$; stimulation intensity: $F(1.4,12.5) = 64.5$, $P < 0.001$; IP injection × stimulation intensity: $F(1,9) = 139.8$, $P < 0.001$], while both paired-pulse ratio (PPR) and coefficient of variation (CV) were significantly reduced in KA-injected as compared with saline-treated mice (Fig. 3*C*) (PPR: saline: 1.31 ± 0.08, $n = 10$; KA: 1.01 ± 0.06, $n = 10$; saline vs. KA: $P = 0.011$, unpaired *t* test; CV: saline: 0.44 ± 0.06, $n = 10$; KA: 0.28 ± 0.02, $n = 10$; saline vs. KA: $P = 0.026$, unpaired *t* test). These results strongly suggest that initial seizures, presumably by inducing presynaptic LTP, strengthened MC-GC synapses in vivo. If so, this plasticity should be occluded in hippocampal slices prepared from KA-injected mice. In support of this possibility, we found that both synaptically induced LTP by repetitive stimulation of MC axons (Fig. 3*D*) (saline: 155.5 ± 14.7% of baseline, $n = 6$, $P = 0.013$, paired *t* test; KA: 99.2 ± 3.8% of baseline, $n = 5$, $P = 0.85$, paired *t* test; saline vs. KA: $P = 0.011$, unpaired *t* test) and chemically induced LTP by transient application (50 μM for 10 min) of the adenylyl-cyclase activator forskolin (23) (Fig. 3*E*) (saline: 170.7 ± 7.6% of baseline, $n = 9$, $P < 0.001$, paired *t* test; KA: 114.3 ± 9.8% of baseline, $n = 6$, $P = 0.20$, paired *t* test; saline vs. KA: $P = 0.0005$, unpaired *t* test) were impaired in KA-injected mice as compared with control (Fig. 3 *D* and *E*). Altogether, our findings strongly suggest that early KA-induced seizures strengthened MC-GC synaptic transmission by inducing presynaptic MC-GC LTP in vivo.

We also examined whether KA-induced seizures could modify medial perforant path (MPP) to GC synaptic transmission (*SI Appendix*, Fig. S3*A*). We found an increase in input/output function and the ratio of α-amino-3-hydroxy-5-methyl-4-isoxazolepropionic acid receptor (AMPA) and N-methyl-D-aspartate receptor (NMDA) EPSCs (AMPA/NMDA ratio) but no change in PPR in KA-injected mice (*SI Appendix*, Fig. S3 *B–D*), suggesting that initial seizures strengthened MPP-GC synapses via a postsynaptic mechanism.

Blocking Seizure-Induced MC-GC LTP Had an Anticonvulsant Effect. BDNF/TrkB signaling is critical for MC-GC LTP. BDNF is released, by both MCs and GCs, upon repetitive presynaptic activity and is necessary and sufficient for the induction of MC-GC LTP (23, 24). To test whether BDNF is also

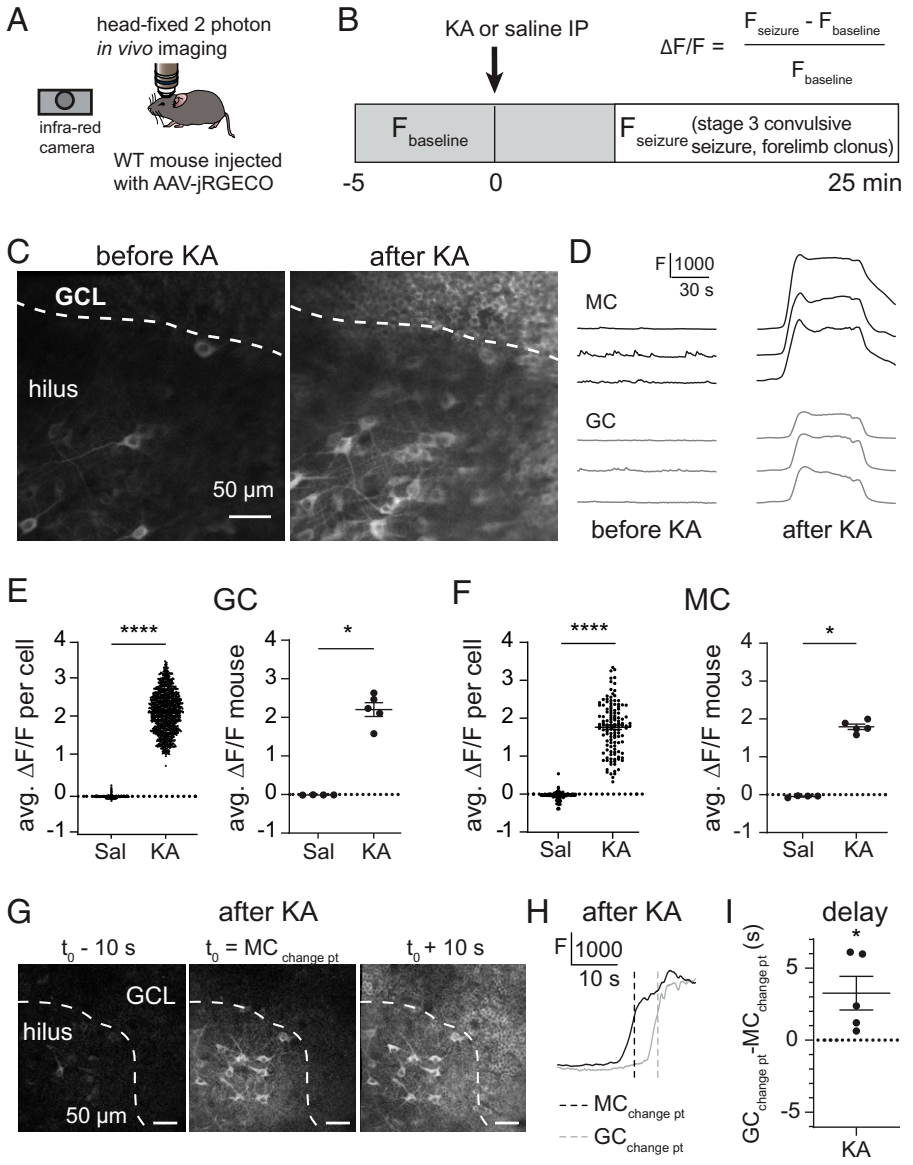

Fig. 2. Initial convulsive seizures increased MC and GC in vivo activity. (*A* and *B*) Schematic diagram showing the experimental apparatus (*A*). jRGECO1a-expressing MCs and GCs were imaged before and during KA (30 mg/kg)–induced convulsive seizures in head-fixed mice monitored with an infrared camera. Saline injections were used as control. (*C*) Mean image, acquired in vivo, of jRGECO1a-expressing MCs (hilus) and GCs (granule cell layer, GCL) before and after KA injection. (*D*) Representative fluorescence (*F*) traces of three individual MCs and GCs before and after KA injection. (*E* and *F*) Average ΔF/F (avg. ΔF/F) of recorded MCs and GCs after saline (Sal) or KA injection. Each data point corresponds to the average value per cell (*Left*) and per animal (*Right*). (*G*) Representative single-frame images acquired during MC activation [mean MC changepoint (change pt) t_0, *Middle*], as well as 10 s before and after (*Left* and *Right*), illustrating how the increase in MC activity, as measured by calcium signals, occurs a few seconds before the increase in GC activity during KA-induced convulsive seizures. (*H*) Representative *F* traces of individual MC (black trace) and GC (gray trace) activation during KA-induced convulsive seizures. Vertical dashed lines indicate changepoints for MC and GC. MCs were activated before GCs. (*I*) Summary plot showing the delay ($GC_{changepoint} - MC_{changepoint}$) in GC and MC activation, averaged by mouse. *$P < 0.5$, ****$P < 0.0001$. Data are presented as mean ± SEM.

involved in the seizure-induced strengthening of MC-GC synaptic transmission, occurring in vivo, we conditionally knocked out *Bdnf* from GCs, a manipulation that abolishes MC-GC LTP (24), and tested whether seizures can trigger MC-GC potentiation in absence of postsynaptic BDNF. Given that experimental seizures can be reduced in *Bdnf* KO mice (33, 34), we only injected 0.5 μL of AAV5.CaMKII.Cre-mCherry or AAV5.CaMKII.mCherry (control) into the DG upper blade of $Bdnf^{fl/fl}$ mice unilaterally (*SI Appendix*, Fig. S4 *A* and *B*) in order to prevent a potential failure in seizure induction when knocking out *Bdnf* from DG excitatory neurons. Mice were killed humanely 25 min after KA injection, which is the average time for reaching stage 3 convulsive seizure in WT control mice. We then prepared acute slices to monitor MC-GC synaptic function (Fig. 4*A*). While behavioral seizures were comparable in control and cKO mice (all animals reached stage 3 of convulsive seizures and no higher at 25 min postinjection), *Bdnf* deletion from GCs (Cre-mCherry$^+$ GCs) prevented seizure-induced MC-GC LTP, as KA IP injection failed to increase MC EPSC amplitude (Fig. 4*B*) [two-way ANOVA RM; IP injection: $F(1,6) = 0.003$, $P = 0.96$; stimulation intensity: $F(1.56,9.38) = 57.97$, $P = 0.0004$; IP injection × stimulation intensity: $F(1,6) = 287.4$, $P < 0.001$] or decrease PPR (Fig. 4*C*) (saline: 1.23 ± 0.01, $n = 7$; KA: 1.25 ± 0.1, $n = 7$; saline vs. KA: $P = 0.90$, unpaired *t* test) and CV (Fig. 4*C*) (saline: 0.40 ± 0.04, $n = 7$; KA: 0.42 ± 0.06, $n = 7$; saline vs. KA: $P = 0.79$, unpaired *t* test) as compared with saline-injected mice. The lack of KA-induced synaptic strengthening was not due to viral expression, since KA injection efficiently increased the input/output function (MC EPSC amplitude, Fig. 4*D*) [two-way ANOVA RM; IP injection:

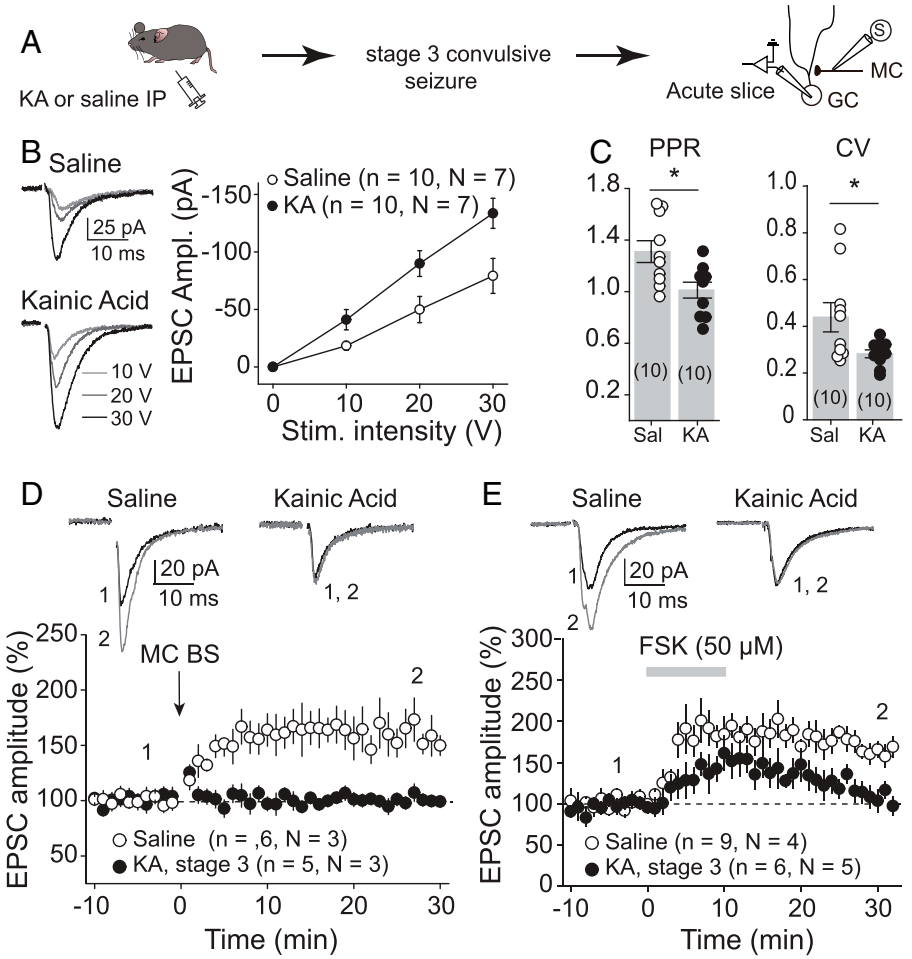

Fig. 3. Initial convulsive seizures increased MC-GC synaptic strength. (*A*) Seizures were acutely induced using KA IP (20 mg/kg). Mice were killed humanely after reaching stage 3 of convulsive seizures, and MC-GC synaptic function was accessed in acute hippocampal slices. Saline-injected mice were used as control. (*B*) Representative traces and summary plot showing how input/output function was increased in KA-injected mice. EPSC amplitude (Ampl.) vs stimulus (Stim.) intensity is plotted. (*C*) PPR and CV were both significantly decreased in KA-treated mice as compared with saline-injected mice. Each number in parentheses represents the number of cells. (*D* and *E*) Representative traces (*Top*) and time course summary plots (*Bottom*) showing that LTP at MC-GC synapses induced by either MC BS (five pulses at 100 Hz, repeated 50 times every 0.5 s, *D*) or 50 µM forskolin (FSK, *E*) application was impaired in KA-injected mice. *$P < 0.5$. Data are presented as mean ± SEM.

$F(1,4) = 23.6$, $P = 0.008$; stimulation intensity: $F(1.34,5.34) = 68.9$, $P = 0.0002$; IP injection × stimulation intensity: $F(1,4) = 537.0$, $P < 0.0001$] and reduced PPR (Fig. 4*E*) (saline: 1.34 ± 0.1, $n = 5$; KA: 0.98 ± 0.1, $n = 7$; saline vs. KA: $P = 0.014$, unpaired t test) and CV (Fig. 4*E*) (saline: 0.39 ± 0.04, $n = 5$; KA: 0.27 ± 0.03, $n = 7$; saline vs. KA: $P = 0.031$, unpaired t test) in mCherry$^+$ control GCs. Deleting *Bdnf* from GCs did not alter MC-GC synaptic function in saline-injected mice, as indicated by the fact that input/output function (Fig. 4 *B* and *D*) [saline: two-way ANOVA RM; AAV: $F(1,4) = 0.27$, $P = 0.63$; stimulation intensity: $F(1.48,5.94) = 75.57$, $P < 0.00001$; AAV × stimulation intensity: $F(1,4) = 174.09$, $P = 0.0002$], PPR (Fig. 4 *C* and *E*) (saline control: 1.34 ± 0.1, $n = 5$; saline cKO: 1.23 ± 0.01, $n = 7$; control vs. cKO: $P = 0.44$, unpaired t test), and CV (Fig. 4 *C* and *E*) (saline control: 0.39 ± 0.04, $n = 5$; saline cKO: 0.40 ± 0.04, $n = 7$; control vs. cKO: $P = 0.91$, unpaired t test) were similar in Cre$^+$ GCs (*Bdnf* cKO) as compared to mCherry$^+$ GCs (control). In contrast, KA-injected mice showed a significant reduction in input/output function (Fig. 4 *B* and *D*) [KA: two-way ANOVA RM; AAV: $F(1,6) = 10.84$, $P = 0.017$; stimulation intensity: $F(1.39,8.38) = 64.08$, $P = 0.00002$; AAV × stimulation intensity: $F(1,6) = 166.81$, $P = 0.00001$] and significant increase in both PPR (Fig. 4 *C* and *E*) (KA control: 0.98 ± 0.1, $n = 7$; KA cKO: 1.25 ± 0.1, $n = 7$; control vs. cKO: $P = 0.049$, unpaired t test) and CV (Fig. 4 *C* and *E*) (KA control: 0.27 ± 0.03, $n = 7$; KA cKO: 0.42 ± 0.06, $n = 7$; control vs. cKO: $P = 0.044$, unpaired t test) in *Bdnf* cKO mice as compared with control animals. GC membrane properties were similar among all of the different groups (*SI Appendix*, Fig. S5).

To directly address a potential confounding reduction of KA-induced seizures in *Bdnf* cKOs (33, 34), we also compared MC-GC synaptic function in Cre$^+$ (*Bdnf* cKO) with Cre$^-$ (control) GCs recorded from the same animal following KA administration (*SI Appendix*, Fig. S4 *A* and *B*). The amplitude of evoked EPSCs was significantly decreased (*SI Appendix*, Fig. S4*C*) and PPR was significantly increased in Cre-expressing GCs as compared with neighboring Cre-lacking GCs (*SI Appendix*, Fig. S4*D*), further supporting the BDNF requirement for the KA-induced MC-GC strengthening. Lastly, *Bdnf* deletion from GCs also reduced the KA-induced strengthening of MPP-GC transmission (*SI Appendix*, Fig. S6). Thus, while *Bdnf* cKO had no impact on basal MC-GC and MPP-GC synaptic transmission and GC membrane properties, it abolished KA-induced strengthening of both MC-GC and MPP-GC synaptic transmission.

Because protein kinase A (PKA) activity is required for MC-GC LTP downstream of BDNF/TrkB signaling (23, 24), we examined whether PKA activation could still induce LTP in

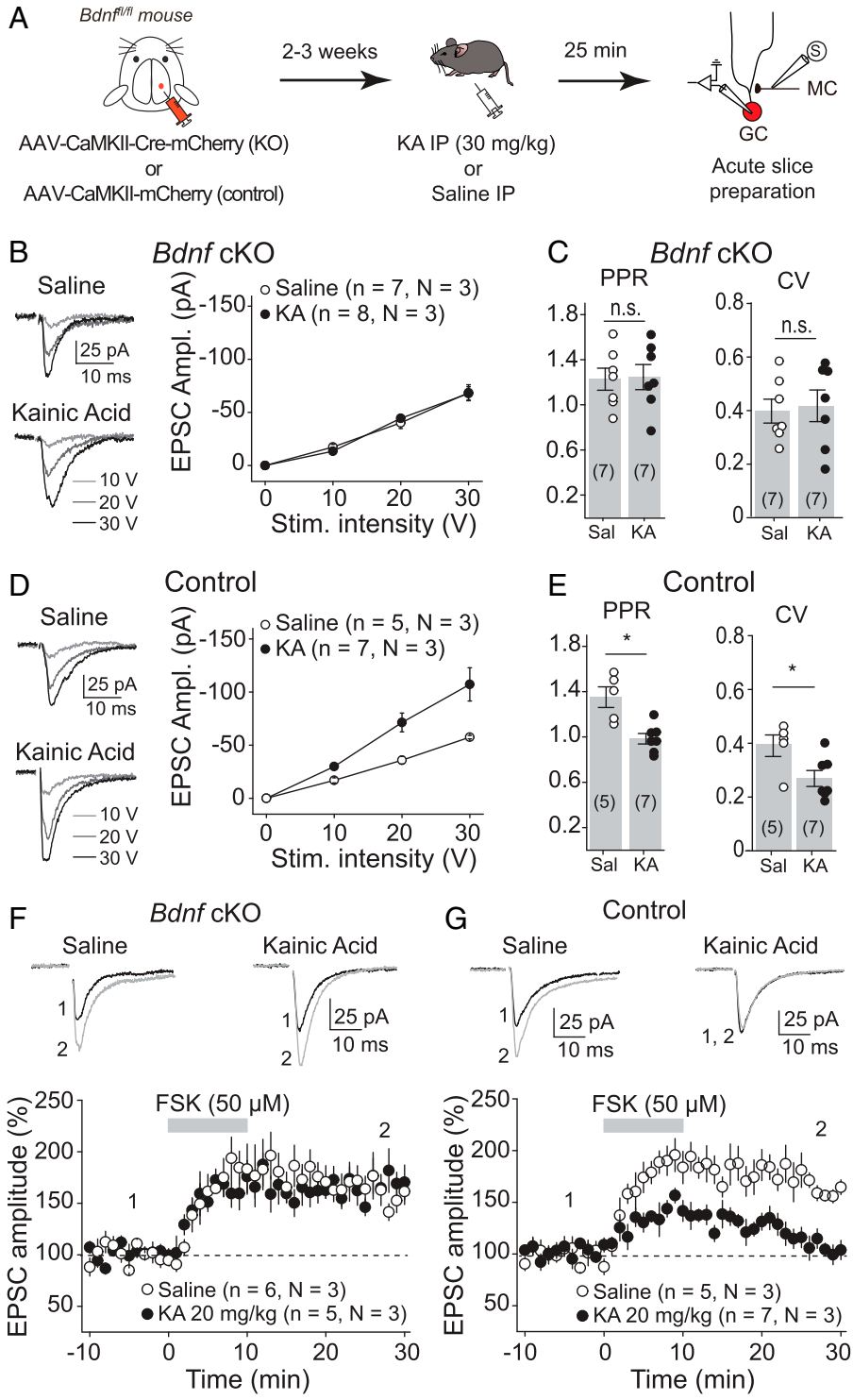

Fig. 4. Seizure-induced MC-GC synaptic strengthening required postsynaptic BDNF. (*A*) Experimental timeline. Control (AAV-CaMKII-mCherry) or Cre-expressing AAV (AAV-CaMKII-Cre-mCherry) were injected unilaterally into the dorsal blade of the DG of *Bdnf*$^{fl/fl}$ mice. Seizures were induced 2 to 3 wk later using KA IP (30 mg/kg), and acute hippocampal slices were prepared 25 min postinjection. Then, whole-cell recordings were performed from mCherry^{+} GC, and synaptic responses were monitored in response to MC axon stimulation. (*B* and *C*) KA-induced seizure failed to increase MC-GC synaptic strength in GC-lacking BDNF. EPSC amplitude (*B*), PPR (*C*), and CV (*C*) were similar in Cre-mCherry^{+} GCs obtained from KA vs. saline-injected mice. (*D* and *E*) Seizure induction increased MC-GC EPSC amplitude (*D*) and decreased PPR and CV (*E*) in control mice. (*F*) Representative traces and time course summary plots showing similar FSK-induced potentiation of evoked MC-GC EPSCs (50 μM FSK bath application for 10 min) recorded from *Bdnf* cKO GCs in KA- and saline-injected mice. (*G*) FSK-induced potentiation of MC-GC synaptic transmission in *Bdnf*$^{fl/fl}$ mice injected with a control virus (AAV-CaMKII-mCherry) was impaired in KA-injected mice (20 mg/kg) as compared with saline-treated mice. *$P < 0.05$; nonsignificant, n.s., $P > 0.05$. Data are presented as mean ± SEM.

BDNF-deficient GCs. Bath application of forskolin (50 μM for 10 min) triggered normal LTP in BDNF-deficient GCs (Cre-mCherry^{+}) obtained from both KA- and saline-injected mice in postsynaptic *Bdnf* cKOs (Fig. 4*F*) (saline: 162.9 ± 9.4% of baseline, $n = 6$, $P = 0.0011$, paired t test; KA: 161.9 ± 5.7% of baseline, $n = 5$, $P = 0.0004$, paired t test; saline vs. KA: $P = 0.85$, unpaired t test), supporting the idea that postsynaptic *Bdnf* deletion prevented KA injection from inducing MC-GC LTP

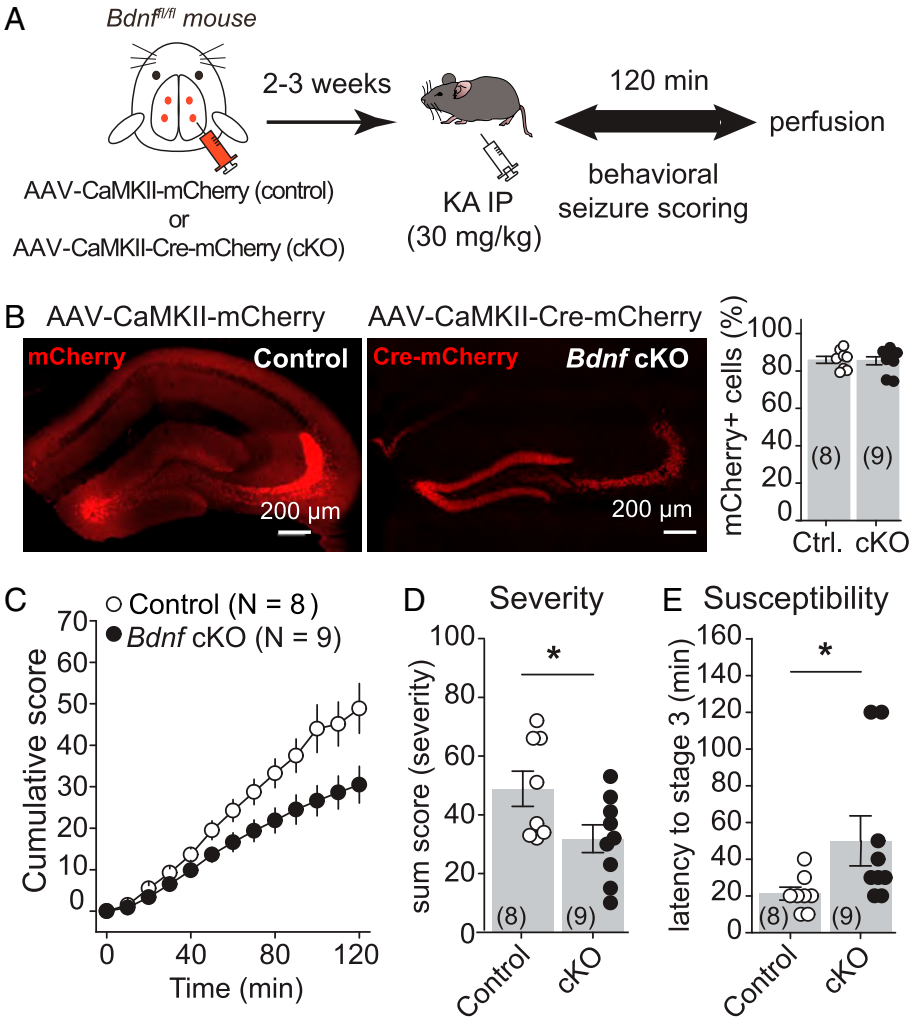

Fig. 5. Knocking out BDNF from hippocampal excitatory neurons reduced KA-induced seizures. (*A*) AAV-CaMKII-mCherry (control) or AAV-CaMKII-Cre-mCherry (cKO) was injected bilaterally into ventral and dorsal DG of *Bdnf*$^{fl/fl}$ mice. (*B*) Representative confocal images (*Left*) and quantification (*Right*) showing high viral expression in the DG. Control (Ctrl) vs cKO. (*C–E*) Deletion of BDNF from hippocampal excitatory neurons (*Bdnf*$^{fl/fl}$ mice injected with AAV-CaMKII-Cre-mCherry) induced significant decreases in the cumulative seizure score (*C*) and in the sum score (*D*) and a significantly increase in latency to convulsive seizures (*E*) as compared with controls (*Bdnf*$^{fl/fl}$ mice injected with AAV-CaMKII-mCherry). *$P < 0.05$. Data are presented as mean ± SEM.

in vivo. In contrast, and consistent with our previous results (Fig. 3*E*), forskolin failed to induce LTP in control GCs (mCherry^{+}) obtained from KA-injected mice but not from saline-injected mice (Fig. 4*G*) (saline: 171.5 ± 7.2% of baseline, $n = 5$, $P = 0.0006$, paired t test; KA: 115.7 ± 8.1% of baseline, $n = 7$, $P = 0.10$, paired t test; saline vs. KA: $P = 0.0006$, unpaired t test). Altogether, these results reveal that initial seizures triggered MC-GC LTP in vivo via a BDNF-dependent mechanism and that such synaptic potentiation occluded subsequent induction of LTP in vitro.

Deleting *Bdnf* from DG excitatory neurons, a manipulation that abolishes MC-GC LTP both in vitro (24) or in vivo (Fig. 4 and *SI Appendix*, Fig. S4), could inhibit seizure induction. To test this possibility, we stereotaxically injected AAV-CaMKII-Cre-mCherry (cKO) or AAV-CaMKII-mCherry (control) into both dorsal and ventral DG of adult *Bdnf*$^{fl/fl}$ mice, bilaterally (Fig. 5*A*). We confirmed that the virus was highly expressed in the DG (Fig. 5*B*) (control: 85.9 ± 1.9% of DG neurons, eight mice; cKO: 85.5 ± 2.1% of DG neurons, nine mice; ∼1,000 analyzed neurons per animal) and that injection of AAV-CaMKII-Cre-mCherry into the hippocampus of *Bdnf*$^{fl/fl}$ mice strongly reduced *Bdnf* mRNA levels selectively in the hippocampus (*SI Appendix*, Fig. S7). *Bdnf* conditional deletion reduced seizure severity and susceptibility, as indicated by significant decreases in the total cumulative seizure score (Fig. 5*C*) [two-way ANOVA RM; AAV condition: $F(1,7) = 6.0$, $P = 0.044$; time: $F(1.26,8.87) = 150.4$, $P < 0.001$; AAV condition × time: $F(1,7) = 262.4$, $P < 0.001$] and in the sum score (Fig. 5*D*) (control: 48.9 ± 6.0, $n = 8$; cKO: 31.7 ± 4.7, $n = 9$; control vs. cKO: $P = 0.039$, unpaired t test) and an increase in latency to stage 3 (Fig. 5*E*) (control: 21.2 ± 3.5, $n = 8$; cKO: 51.1 ± 13.4, $n = 9$; control vs. cKO: $P = 0.045$, Mann–Whitney U test). Remarkably, c-Fos expression was significantly reduced in *Bdnf* cKO mice as compared with controls (*SI Appendix*, Fig. S8). Lastly, we found no significant changes in the amplitude and frequency of spontaneous EPSC (*SI Appendix*, Fig. S9) or in the amplitude of evoked MC-EPSCs (Fig. 4), MPP-EPSCs (*SI Appendix*, Fig. S6*C*), and lateral perforant path (LPP)–EPSCs (*SI Appendix*, Fig. S10) recorded from *Bdnf*-lacking GCs, showing that conditionally knocking out *Bdnf* from DG excitatory neurons did not modify the strength of basal excitatory inputs onto GCs. Altogether, these results indicate that seizure-induced MC-CG LTP accentuates the proconvulsant effects of KA.

In Vivo Application of the MC-GC LTP Induction Protocol Promoted Behavioral Seizures. We previously showed that optogenetic repetitive stimulation of MC axons triggers robust MC-GC LTP in vitro (23). We therefore tested whether in vivo

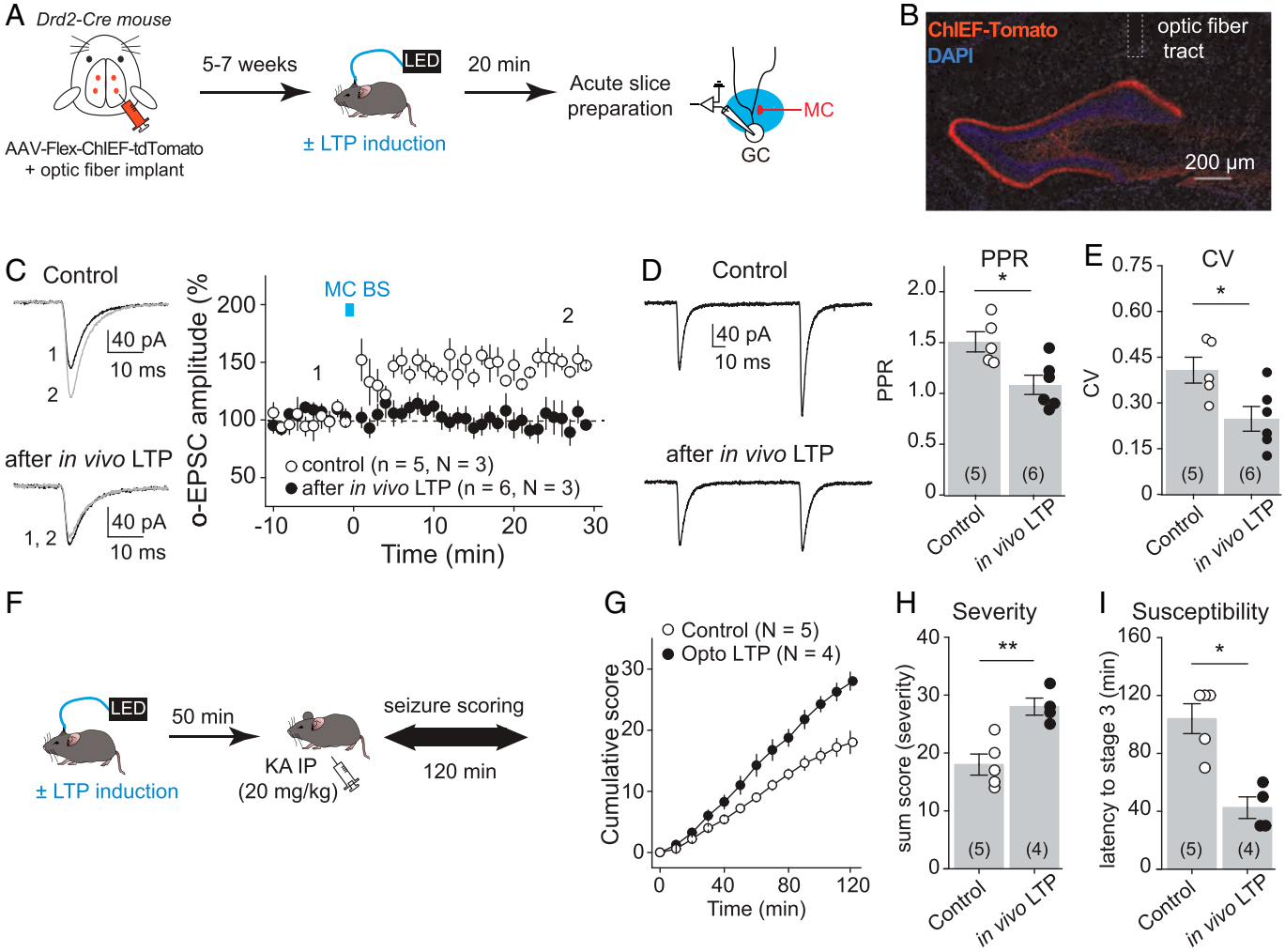

Fig. 6. In vivo induction of MC-GC LTP promoted seizures. (*A*) Experimental timeline. To selectively photostimulate MC axons in vivo, AAV-hSyn-ChIEF-tdTomato was bilaterally injected into ventral and dorsal DG of *Drd2*-cre mice, and an optical fiber was implanted above the IML of the DG. The LTP induction protocol (MC BS: five pulses at 30 Hz, repeated 50 times, every 0.5 s) was applied in vivo by delivering blue light through a patch cord cable connected to a fiber-coupled 470-nm light-emitting diode (LED) source 5 to 7 wk after surgery. Sham light was used as a control. Acute hippocampal slices were prepared 20 min later, and MC-GC synaptic properties were analyzed using whole-cell recordings of GCs and light stimulation of MC axons. (*B*) Representative confocal images showing the viral expression and the fiber tract location. (*C*) Optically evoked EPSCs (o-EPSCs) were recorded in GC in response to MC axon photostimulation. Representative traces (light) and time course summary plot (light) showing that in vivo application of MC BS prevented subsequent induction of LTP in vitro. (*D* and *E*) PPR (*D*) and CV (*E*) were both significantly decreased after in vivo application of the MC-GC LTP induction protocol as compared with the sham light (control) condition. Each number in parentheses indicates the number of cells. (*F*) Experimental timeline. The LTP induction protocol (MC BS: five pulses at 30 Hz, repeated 50 times, every 0.5 s) was delivered in vivo, while sham light was used as control. KA (20 mg/kg IP) was then administered 50 min after the optogenetic stimulation, and seizures were scored for 120 min. (*G–I*) Application of the MC-GC LTP induction protocol (optogenetically-induced LTP or Opto LTP) increased seizure severity and susceptibility, as indicated by significant increases in the cumulative seizure score (*G*) and in the sum score (*H*) and a significantly decrease in latency to convulsive seizures (*I*). $^{*}P < 0.05$, $^{**}P < 0.01$. Data are presented as mean ± SEM.

induction of LTP using optogenetic activation of MCs facilitated acutely evoked behavioral seizures. To this end, we selectively expressed the fast variant of channelrhodopsin ChIEF in MCs by bilaterally injecting the Cre-recombinase–dependent AAV-hSyn-DIO-ChIEF-tdTomato into the dorsal and ventral DG of *Drd2*-Cre mice (Fig. 6*A*). Blue light burst stimulation of MC axons (MC BS: five pulses of 5 ms at 30 Hz, repeated 50 times every 0.5 s) was delivered through an optic fiber placed above the dorsal DG inner molecular layer (IML) in vivo, and sham light (i.e., no light) was used as a control (Fig. 6 *A*, *B*, and *F*). Optic fiber location and selective viral expression in MCs were confirmed post hoc (Fig. 6*B*). We also verified that the light stimulation protocol induced MC-GC LTP in vivo. When it does, this plasticity should be occluded in hippocampal slices prepared after in vivo light stimulation. We found that repetitive light stimulation of MC axons failed to induce LTP in vitro when the LTP protocol was preapplied in vivo as compared with control slices (Fig. 6*C*) (after in vivo LTP: 96.1 ± 7.9% of baseline, $n = 6$, $P = 0.64$, paired t test; control: 146.7 ± 4.9% of baseline, $n = 5$, $P = 0.0007$, paired t test; in vivo LTP vs. control: $P < 0.001$, unpaired t test). In addition, both PPR (Fig. 6*D*) (control: 1.51 ± 0.10, $n = 5$; in vivo LTP: 1.08 ± 0.09, $n = 6$; control vs. in vivo LTP: $P = 0.013$, unpaired t test) and CV (Fig. 6*E*) (control: 0.41 ± 0.04, $n = 5$; in vivo LTP: 0.25 ± 0.04, $n = 6$; control vs. in vivo LTP: $P = 0.024$, unpaired t test) were significantly reduced after in vivo photostimulation as compared with control mice (sham light). These results strongly suggest that in vivo MC BS (five pulses of 5 ms at 30 Hz, repeated 50 times every 0.5 s) induced presynaptic LTP at MC-GC synapses. We then tested whether in vivo induction of MC-GC LTP can promote behavioral seizures. In these experiments, to facilitate the detection of potential increase in seizure severity/susceptibility, seizures were induced with a lower dose of KA IP (20 mg/kg) 50 min after in vivo induction of LTP (Fig. 6*F*). Remarkably, we

found that in vivo application of a MC-GC LTP induction protocol significantly increased the severity and susceptibility of acutely evoked seizures induced by KA, as indicated by significant increases in cumulative seizure score (Fig. 6*G*) [two-way ANOVA RM; light: $F(1,3) = 100.7$, $P < 0.001$; time: $F(1.3,4.1) = 221.5$, $P < 0.001$; light × time: $F(1,3) = 109.3$, $P < 0.01$] and in the sum score (Fig. 6*H*) (control: 18.0 ± 1.8, $n = 5$; in vivo LTP: 28.0 ± 1.5, $n = 4$; control vs. in vivo LTP: $P = 0.0045$, unpaired t test) and a significantly decrease in latency to convulsive seizures (Fig. 6*I*) (control: 104.0 ± 10.3, $n = 5$; in vivo LTP: 42.5 ± 7.5, $n = 4$; control vs. in vivo LTP: $P = 0.017$, Mann–Whitney U test). While optogenetic activation of MCs could impact their basic membrane properties or synaptic inputs, we found that the stimulation protocol that triggers LTP in vivo did not significantly alter MC membrane resistance or the main excitatory synaptic drive, i.e., GC inputs, onto MC recorded in vitro (*SI Appendix*, Fig. S11) (see *Materials and Methods*). Taken together, these findings strongly suggest that in vivo induction of MC-GC LTP can worsen behavioral seizures.

Discussion

In this study, we found that early seizures potentiate crucial hippocampal excitatory synapses, thereby facilitating further epileptic activity. KA-induced seizures not only increased MC and GC activity in vivo but also triggered a BDNF-dependent strengthening of MC-GC synaptic transmission that occluded subsequent induction of MC-GC LTP. In addition, blocking MC-GC LTP and silencing MCs selectively were both associated with significant decreases in seizure susceptibility and severity. Moreover, in vivo induction of MC-GC LTP was sufficient to worsen convulsive seizures subsequently triggered with KA. Overall, our findings strongly suggest that seizure-induced plasticity at MC-GC excitatory synapses may significantly contribute to the proconvulsant role of MCs during early stages of epilepsy.

Initial Seizures Induce BDNF-Dependent Strengthening of MC-GC Synaptic Transmission. Using in vivo two-photon imaging in awake behaving mice, we found that acutely induced seizures triggered a massive increase in both MC and GC calcium signals (Fig. 2), indicating a robust increase in neuronal activity. Our findings are consistent with a recent study reporting in vivo epileptiform calcium signals detected with fiber photometry in the DG following KA administration (32). While these signals likely reflect the synchronized activity of a large population of neurons, including interneurons, we could assess calcium activity of individual MCs and GCs (Fig. 2 and *SI Appendix*, Fig. S2 *D* and *E*) by combining selective expression of a calcium indicator in DG excitatory neurons and two-photon live imaging. It has been reported that dorsal GCs are mainly activated by ventral MCs (31), which we were not able to confirm given the limited access to the ventral hippocampus of our head-fixed two-photon imaging approach. However, imaging of the dorsal hippocampus revealed that MC activation during convulsion seizures precedes GCs (Fig. 2 *G*–*I*). We therefore hypothesize that KA administration activates MCs, which in turn engage GCs. In support of this idea, we have recently reported that MCs express functional extrasynaptic kainate receptors whose activation with submicromolar concentrations of KA can drive MC activity in vitro, whereas GCs show comparatively much less sensitivity (at least one order of magnitude) to KA application (35). While interneurons (36) and CA3 pyramidal cells also express kainate receptors (37, 38), it is unlikely that activation of these neurons could directly drive GCs, although CA3 pyramidal cells could contribute indirectly by activating MCs (39). Furthermore, MCs show higher activity in vivo in contrast to GCs (40–42), making them more likely to be engaged during epileptic activity, regardless the nature of the chemoconvulsant. This last notion is also supported by the fact that MC silencing not only reduced KA-induced seizures (Fig. 1) but also prevents pilocarpine-induced epilepsy (5). Although MCs also excite inhibitory interneurons (16), the anticonvulsant effect of MC silencing (Fig. 1) suggests that MC silencing during initial seizures has a stronger impact on the activity of GCs than interneurons (5). Besides inducing synaptic plasticity, the KA-induced increase in MC and GC intracellular calcium concentration (Fig. 2) may also contribute to excitotoxicity and cell death. Altogether, our findings demonstrate that MCs and GCs are highly active during initial experimental seizures, suggesting that sustained activation of MCs contributes to GC recruitment.

We gathered multiple lines of evidence indicating that initial convulsive seizures induce presynaptically expressed MC-GC LTP in vivo. MC-GC synaptic strength was increased in KA-treated mice as compared with sham-injected animals, and this strengthening was associated with a significant reduction in both PPR and CV (Fig. 3 *B* and *C*), suggesting a presynaptic mechanism. Moreover, induction of MC-GC LTP in vitro was occluded after convulsive seizures (Fig. 3 *D* and *E*), indicating a common step. The KA-induced strengthening of MC-GC synaptic transmission in vivo was likely induced by the increase in MC activity (35), consistent with the observation that repetitive MC activity triggers robust MC-GC LTP in acute rodent hippocampal slices (23). Although in vitro epileptic activity was associated with a rise in the net excitatory drive between MCs and GCs (5), it is unclear whether this effect results from disinhibition or direct MC-GC synaptic strengthening. Our findings show that both in vivo optogenetic activation of MCs (Fig. 6) and acute seizures (Fig. 3) were sufficient to trigger presynaptic MC-GC LTP.

Several studies indicate that seizures can increase both BDNF levels (43–46) and TrkB activation in the hippocampus (25, 47). In addition, BDNF is necessary and sufficient for MC-GC LTP (23), and it can be released from both MCs and GCs following MC repetitive activity in vitro (24). It is therefore likely that by releasing BDNF, MC and GC activity induces MC-GC LTP in vivo. In support of this mechanism, we found that genetic removal of *Bdnf* from GCs abolished seizure-induced MC-GC LTP (Fig. 4 and *SI Appendix*, Fig. S4), while it did not affect basal MC-GC synaptic (Fig. 3) or GC membrane properties in sham-injected mice (*SI Appendix*, Fig. S5). Of note, we did not observe any failure of seizure induction when *Bdnf* was sparsely knocked out. Altogether, our findings indicate that BDNF mediates in vivo seizure-induced strengthening of MC-GC excitatory synapses.

Seizure-Induced LTP at MC-GC Synapses is Proconvulsant. Our results strongly suggest that activity-dependent strengthening of MC-GC synapses promotes acute seizures. While MCs innervate GCs and inhibitory interneurons, MC repetitive activity that induces MC-GC LTP, at least in vitro, has no effect on feedforward inhibition onto GCs (23), and such repetitive activity does not induce plasticity at GC-MC synapses (*SI Appendix*, Fig. S11). LTP-induced worsening of seizures (Fig. 6) is supported by the extensive MC projection onto the proximal dendrites of GCs (16) and the powerful MC-GC excitatory drive reported both in vitro (23) and in vivo (31). Given that a single MC innervates as much as 75% of the septotemporal axis of the hippocampus (48), broad induction of MC-GC LTP can be detrimental,

underscoring a link between uncontrolled LTP at the hippocampal excitatory synapse and seizures. Conversely, blocking activity-dependent strengthening of MC-GC synapses in vivo reduced induced seizure severity. PKA and BDNF signaling pathways are both necessary and sufficient for activity-dependent LTP at MC-GC synapses (23, 24). Both MC silencing using G_i iDREADD (Fig. 1) and knocking out *Bdnf* from hippocampal excitatory neurons (Fig. 5) reduced acute KA-induced seizure severity. However, MC silencing not only prevents MC-GC LTP induction but also reduces basal MC-GC synaptic transmission (Fig. 1) and MC output activity. Although *Bdnf* cKO had no effect on MC-GC basal transmission (Fig. 4) and GC membrane properties (*SI Appendix*, Fig. S5), we cannot discard an effect on other synapses. In fact, we found that deleting *Bdnf* from GCs did not alter MPP- and LPP-GC synaptic transmission (*SI Appendix*, Figs. S6, S9, and S10) but prevented KA-induced MPP-GC strengthening (*SI Appendix*, Fig. S6). A potential role of MC-GC LTP in this strengthening cannot be discarded. *Bdnf* deletion reduced c-Fos expression in the DG of KA-injected mice (*SI Appendix*, Fig. S8), suggesting that BDNF/TrkB signaling contributes to seizure-induced opening of the DG gate, likely by strengthening MC-GC synapses. Consistent with this scenario, optogenetic induction of MC-GC LTP in vivo was sufficient to worsen convulsive seizures. Notably, type 1 cannabinoid receptors, which are highly expressed at MC terminals (49), tonically suppress MC-GC transmission and also dampen the induction of MC-GC LTP (50) in an activity-dependent manner. By suppressing excitatory drive, these receptors could be a potential target to prevent epilepsy (14, 51–53). In agreement with recent findings using the pilocarpine model (5), our results strongly support a proconvulsant role of MCs during early epilepsy. In contrast, in a chronic mouse model of TLE induced by KA intrahippocampal administration, MCs are reportedly antiepileptic (4), suggesting that the role of MCs may differ significantly with the disease stage. A change in MC connectivity that leads to a reduced excitatory/inhibitory drive of GCs could underlie the antiepileptic role of surviving MCs in chronic epilepsy (54).

Compelling evidence indicates that BDNF and its high-affinity receptor TrkB promote worsening of TLE (25, 33, 34, 55–59), but the precise mechanisms and specific contributions of different cell types are not entirely clear. Here we identified two reciprocally connected excitatory neurons in the DG, MCs and GCs, that can mediate the BDNF proconvulsant effects via BDNF-dependent MC-GC LTP. Interfering with BDNF/TrkB signaling in different ways reduced epilepsy—i.e. heterozygous deletion of *Bdnf* (33), neuronal deletion of *Bdnf* or *TrkB* (34), chemogenetic blockade of TrkB kinase activity in $TrkB^{F616A}$ mutant mice (58), and a mutant mouse that uncouples TrkB from its downstream phospholipase Cγ1 signaling (56). Importantly, based on our previous (23) and present (Figs. 4 and 6) findings, these manipulations could also prevent seizure-induced MC-GC LTP and the associated facilitation of epileptic activity. Conversely, overexpression of BDNF in the brain (59) and local infusion of BDNF into the hippocampus (55) worsen epileptic seizures. BDNF is sufficient to induce MC-GC LTP in vitro (23), raising the possibility that in vivo infusion of BDNF promotes seizures by inducing MC-GC LTP broadly. Of note, exogenous BDNF delivery into the hippocampus of chronically epileptic rats can have antiepileptic and neuroprotective effects (60), suggesting that BDNF action might differ with epilepsy stages.

Altogether, our findings uncover a potential mechanism implicated in the early stages of epilepsy before brain damage becomes irreversible. We highlighted how initial seizures can shape an important hippocampal excitatory synapse in a BDNF-dependent manner, and how broad, uncontrolled induction of LTP can be detrimental and promote subsequent induction of seizures. Manipulations that suppress LTP induction and BDNF signaling at MC-GC synapses may be a strategy for the treatment of epilepsy.

Materials and Methods

C57BL/6, *Bdnf* floxed ($Bdnf^{fl/fl}$), or *Drd2*-cre (B6.FVB(Cg)-Tg(*Drd2*-cre)ER44Gsat/Mmucd, MMRRC 032108-UCD) mice (2 to 3.5 mo old, both males and females) were used in this study. All animals were group housed in a standard 12:12 h light:dark cycle and had free access to food and water. Animal handling, breeding, and use followed a protocol approved by the Animal Care and Use Committee of the Albert Einstein College of Medicine, in accordance with NIH guidelines. Experimental procedures, involving hippocampal slice preparation, electrophysiology, in vivo two-photon imaging, *Bdnf* conditional KO (cKO), MC silencing, in vivo induction of MC-GC LTP with optogenetics, seizure induction and monitoring, immunohistochemistry, fluorescent in situ hybridization, and adeno-associated virus vector construction, were detailed in *SI Appendix, Supplementary Materials and Methods*. Image acquisition, quantification, data, and statistical analysis are also included in *SI Appendix, Supplementary Materials and Methods*.

For more details, refer to *SI Appendix, Supplementary Materials and Methods*.

Data Availability. All study data are included in the article and/or *SI Appendix*. Original code was uploaded to GitHub (https://github.com/GoncalvesLab/Nasrallah-et-al-PNAS-2022-Collab) (61). Plasmids generated for this study have been deposited on AddGene (190240, 190241) (62, 63).

ACKNOWLEDGMENTS. We thank the members of the P.E.C. laboratory for constructive feedback, especially Coralie Berthoux and Czarina Ramos for critical reading of the manuscript. We also thank Pascal Kaeser (Harvard University) for sharing an AAV-hSyn-Flex-ChIEF-tdTomato plasmid and Lisa Monteggia (Vanderbilt University) for sharing $Bdnf^{fl/fl}$ mice. This research was supported by the NIH grants R01-NS113600, R01-MH125772, R01-NS115543 and R01-MH116673 to P.E.C., and R21-MH120496 to Y.J.Y.; the Fondation pour la Recherche Médicale (Postdoctoral Fellowship for research abroad), the Fondation Bettencourt Schueller award (Prix pour les Jeunes Chercheurs 2016), and the American Epilepsy Society Postdoctoral Research Fellowship (2020) to K.N.; the Einstein Training Program in Stem Cell Research from the Empire State Stem Cell Fund through New York State Department of Health Contract C34874GG to M.A.F.; and a Whitehall Foundation Research Grant (2019-05-71) to J.T.G. Confocal images were obtained at the Einstein Imaging Core (supported by the Rose F. Kennedy Intellectual Disabilities Research Center, NIH Shared Instrument Grant 1S10OD25295 to Konstantin Dobrenis), and fluorescent in situ hybridization in brain slices was performed using a PerkinElmer P250 high-capacity slide scanner (Shared Instrument Grant 1S10OD019961) at the Einstein Analytical Imaging Facility (supported by Cancer Center Support Grant P30 CA0133330).

Author affiliations: [a]Dominick P. Purpura Department of Neuroscience, Albert Einstein College of Medicine, Bronx, NY 10461; [b]Gottesman Institute for Stem Cell Biology and Regenerative Medicine, Albert Einstein College of Medicine, Bronx, NY 10461; [c]Department of Anatomy and Structural Biology, Albert Einstein College of Medicine, Bronx, NY 10461; and [d]Department of Psychiatry & Behavioral Sciences, Albert Einstein College of Medicine, Bronx, NY 10461

1. R. S. Fisher *et al.*, ILAE official report: A practical clinical definition of epilepsy. *Epilepsia* **55**, 475–482 (2014).
2. M. Bialer *et al.*, Progress report on new antiepileptic drugs: A summary of the Thirteenth Eilat conference on new antiepileptic drugs and devices (EILAT XIII). *Epilepsia* **58**, 181–221 (2017).
3. H. E. Scharfman, The enigmatic mossy cell of the dentate gyrus. *Nat. Rev. Neurosci.* **17**, 562–575 (2016).
4. A. D. Bui *et al.*, Dentate gyrus mossy cells control spontaneous convulsive seizures and spatial memory. *Science* **359**, 787–790 (2018).
5. J. J. Botterill *et al.*, An excitatory and epileptogenic effect of dentate gyrus mossy cells in a mouse model of epilepsy. *Cell Rep.* **29**, 2875–2889.e6 (2019).
6. B. S. Chang, D. H. Lowenstein, Epilepsy. *N. Engl. J. Med.* **349**, 1257–1266 (2003).

7. S. Jinde *et al.*, Hilar mossy cell degeneration causes transient dentate granule cell hyperexcitability and impaired pattern separation. *Neuron* **76**, 1189–1200 (2012).
8. Ad. Ratzliff, V. Santhakumar, A. Howard, I. Soltesz, Mossy cells in epilepsy: Rigor mortis or vigor mortis? *Trends Neurosci.* **25**, 140–144 (2002).
9. I. Blümcke *et al.*, Loss of hilar mossy cells in Ammon's horn sclerosis. *Epilepsia* **41** (suppl. 6), S174–S180 (2000).
10. J. H. Margerison, J. A. Corsellis, Epilepsy and the temporal lobes. A clinical, electroencephalographic and neuropathological study of the brain in epilepsy, with particular reference to the temporal lobes. *Brain* **89**, 499–530 (1966).
11. L. Seress *et al.*, Survival of mossy cells of the hippocampal dentate gyrus in humans with mesial temporal lobe epilepsy. *J. Neurosurg.* **111**, 1237–1247 (2009).
12. B. E. Swartz *et al.*, Hippocampal cell loss in posttraumatic human epilepsy. *Epilepsia* **47**, 1373–1382 (2006).
13. P. S. Buckmaster, A. L. Jongen-Rêlo, Highly specific neuron loss preserves lateral inhibitory circuits in the dentate gyrus of kainate-induced epileptic rats. *J. Neurosci.* **19**, 9519–9529 (1999).
14. Y. Sugaya *et al.*, Crucial roles of the endocannabinoid 2-arachidonoylglycerol in the suppression of epileptic seizures. *Cell Rep.* **16**, 1405–1415 (2016).
15. R. K. Wong, R. D. Traub, R. Miles, Cellular basis of neuronal synchrony in epilepsy. *Adv. Neurol.* **44**, 583–592 (1986).
16. P. S. Buckmaster, H. J. Wenzel, D. D. Kunkel, P. A. Schwartzkroin, Axon arbors and synaptic connections of hippocampal mossy cells in the rat in vivo. *J. Comp. Neurol.* **366**, 271–292 (1996).
17. D. G. Amaral, H. E. Scharfman, P. Lavenex, The dentate gyrus: Fundamental neuroanatomical organization (dentate gyrus for dummies). *Prog. Brain Res.* **163**, 3–22 (2007).
18. D. A. Henze, L. Wittner, G. Buzsáki, Single granule cells reliably discharge targets in the hippocampal CA3 network in vivo. *Nat. Neurosci.* **5**, 790–795 (2002).
19. A. J. Pernía-Andrade, P. Jonas, Theta-gamma-modulated synaptic currents in hippocampal granule cells in vivo define a mechanism for network oscillations. *Neuron* **81**, 140–152 (2014).
20. M. Diamantaki, M. Frey, P. Berens, P. Preston-Ferrer, A. Burgalossi, Sparse activity of identified dentate granule cells during spatial exploration. *eLife* **5**, e20252 (2016).
21. E. Krook-Magnuson *et al.*, In vivo evaluation of the dentate gate theory in epilepsy. *J. Physiol.* **593**, 2379–2388 (2015).
22. D. Hsu, The dentate gyrus as a filter or gate: A look back and a look ahead. *Prog. Brain Res.* **163**, 601–613 (2007).
23. Y. Hashimotodani *et al.*, LTP at Hilar Mossy cell-dentate granule cell synapses modulates dentate gyrus output by increasing excitation/inhibition balance. *Neuron* **95**, 928–943.e3 (2017).
24. C. Berthoux, K. Nasrallah, P. E. Castillo, BDNF-induced BDNF release mediates long-term potentiation. bioRxiv [Preprint] (2021). https://doi.org/10.1101/2021.1230.474558. Accessed 30 December 2021.
25. T. W. Lin, S. C. Harward, Y. Z. Huang, J. O. McNamara, Targeting BDNF/TrkB pathways for preventing or suppressing epilepsy. *Neuropharmacology* **167**, 107734 (2020).
26. J. A. French *et al.*, Characteristics of medial temporal lobe epilepsy: I. Results of history and physical examination. *Ann. Neurol.* **34**, 774–780 (1993).
27. M. Raspall-Chaure, R. F. Chin, B. G. Neville, R. C. Scott, Outcome of paediatric convulsive status epilepticus: A systematic review. *Lancet Neurol.* **5**, 769–779 (2006).
28. A. Pitkänen, K. Lukasiuk, Mechanisms of epileptogenesis and potential treatment targets. *Lancet Neurol.* **10**, 173–186 (2011).
29. M. Lévesque, M. Avoli, The kainic acid model of temporal lobe epilepsy. *Neurosci. Biobehav. Rev.* **37**, 2887–2899 (2013).
30. E. Rusina, C. Bernard, A. Williamson, The kainic acid models of temporal lobe epilepsy. *eNeuro* **8**, ENEURO.0337-20.2021 (2021).
31. F. Fredes *et al.*, Ventro-dorsal hippocampal pathway gates novelty-induced contextual memory formation. *Curr. Biol.* **31**, 25–38.e5 (2021).
32. X. Zhang *et al.*, Stereotypical patterns of epileptiform calcium signal in hippocampal CA1, CA3, dentate gyrus and entorhinal cortex in freely moving mice. *Sci. Rep.* **9**, 4518 (2019).
33. M. Kokaia *et al.*, Suppressed epileptogenesis in BDNF mutant mice. *Exp. Neurol.* **133**, 215–224 (1995).
34. X. P. He *et al.*, Conditional deletion of TrkB but not BDNF prevents epileptogenesis in the kindling model. *Neuron* **43**, 31–42 (2004).
35. C. Ramos *et al.*, Activation of extrasynaptic kainate receptors drives hilar mossy cell activity. *J Neurosci.* **42**, 2872–2884 (2022).
36. M. Frerking, R. C. Malenka, R. A. Nicoll, Synaptic activation of kainate receptors on hippocampal interneurons. *Nat. Neurosci.* **1**, 479–486 (1998).
37. P. E. Castillo, R. C. Malenka, R. A. Nicoll, Kainate receptors mediate a slow postsynaptic current in hippocampal CA3 neurons. *Nature* **388**, 182–186 (1997).
38. C. Mulle *et al.*, Altered synaptic physiology and reduced susceptibility to kainate-induced seizures in GluR6-deficient mice. *Nature* **392**, 601–605 (1998).
39. H. E. Scharfman, The CA3 "backprojection" to the dentate gyrus. *Prog. Brain Res.* **163**, 627–637 (2007).
40. N. B. Danielson *et al.*, In vivo imaging of dentate gyrus mossy cells in behaving mice. *Neuron* **93**, 552–559.e4 (2017).
41. D. GoodSmith *et al.*, Spatial representations of granule cells and mossy cells of the dentate gyrus. *Neuron* **93**, 677–690.e5 (2017).
42. Y. Senzai, G. Buzsáki, Physiological properties and behavioral correlates of hippocampal granule cells and mossy cells. *Neuron* **93**, 691–704.e5 (2017).
43. J. C. Lauterborn *et al.*, Differential effects of protein synthesis inhibition on the activity-dependent expression of BDNF transcripts: Evidence for immediate-early gene responses from specific promoters. *J. Neurosci.* **16**, 7428–7436 (1996).
44. C. Humpel *et al.*, Monitoring release of neurotrophic activity in the brains of awake rats. *Science* **269**, 552–554 (1995).
45. D. H. Lowenstein, M. S. Seren, F. M. Longo, Prolonged increases in neurotrophic activity associated with kainate-induced hippocampal synaptic reorganization. *Neuroscience* **56**, 597–604 (1993).
46. D. K. Binder, S. D. Croll, C. M. Gall, H. E. Scharfman, BDNF and epilepsy: Too much of a good thing? *Trends Neurosci.* **24**, 47–53 (2001).
47. D. K. Binder, M. J. Routbort, J. O. McNamara, Immunohistochemical evidence of seizure-induced activation of trk receptors in the mossy fiber pathway of adult rat hippocampus. *J. Neurosci.* **19**, 4616–4626 (1999).
48. D. G. Amaral, M. P. Witter, The three-dimensional organization of the hippocampal formation: A review of anatomical data. *Neuroscience* **31**, 571–591 (1989).
49. I. Katona *et al.*, Molecular composition of the endocannabinoid system at glutamatergic synapses. *J. Neurosci.* **26**, 5628–5637 (2006).
50. K. R. Jensen, C. Berthoux, K. Nasrallah, P. E. Castillo, Multiple cannabinoid signaling cascades powerfully suppress recurrent excitation in the hippocampus. *Proc. Natl. Acad. Sci. U.S.A.* **118**, e2017590118 (2021).
51. G. Marsicano *et al.*, CB1 cannabinoid receptors and on-demand defense against excitotoxicity. *Science* **302**, 84–88 (2003).
52. K. Monory *et al.*, The endocannabinoid system controls key epileptogenic circuits in the hippocampus. *Neuron* **51**, 455–466 (2006).
53. I. Katona, Cannabis and endocannabinoid signaling in epilepsy. *Handb. Exp. Pharmacol.* **231**, 285–316 (2015).
54. C. R. Butler, G. L. Westbrook, E. Schnell, Adaptive mossy cell circuit plasticity after status epilepticus. *J. Neurosci.* **42**, 3025–3036 (2022).
55. H. E. Scharfman, J. H. Goodman, A. L. Sollas, S. D. Croll, Spontaneous limbic seizures after intrahippocampal infusion of brain-derived neurotrophic factor. *Exp. Neurol.* **174**, 201–214 (2002).
56. X. P. He, E. Pan, C. Sciarretta, L. Minichiello, J. O. McNamara, Disruption of TrkB-mediated phospholipase Cgamma signaling inhibits limbic epileptogenesis. *J. Neurosci.* **30**, 6188–6196 (2010).
57. C. Heinrich *et al.*, Increase in BDNF-mediated TrkB signaling promotes epileptogenesis in a mouse model of mesial temporal lobe epilepsy. *Neurobiol. Dis.* **42**, 35–47 (2011).
58. G. Liu *et al.*, Transient inhibition of TrkB kinase after status epilepticus prevents development of temporal lobe epilepsy. *Neuron* **79**, 31–38 (2013).
59. S. D. Croll *et al.*, Brain-derived neurotrophic factor transgenic mice exhibit passive avoidance deficits, increased seizure severity and in vitro hyperexcitability in the hippocampus and entorhinal cortex. *Neuroscience* **93**, 1491–1506 (1999).
60. C. Falcicchia *et al.*, Seizure-suppressant and neuroprotective effects of encapsulated BDNF-producing cells in a rat model of temporal lobe epilepsy. *Mol. Ther. Methods Clin. Dev.* **9**, 211–224 (2018).
61. K. Nasrallah *et al.*, Data from "Seizure-induced strengthening of a recurrent excitatory circuit in the dentate gyrus is proconvulsant." GitHub. https://github.com/GoncalvesLab/Nasrallah-et-al-PNAS-2022-Collab. Deposited 21 July 2022.
62. K. Nasrallah *et al.*, Plasmid from "Seizure-induced strengthening of a recurrent excitatory circuit in the dentate gyrus is proconvulsant." AddGene. http://www.addgene.org/search/advanced/?q=190240. Deposited 3 August 2022.
63. K. Nasrallah *et al.*, Plasmid from "Seizure-induced strengthening of a recurrent excitatory circuit in the dentate gyrus is proconvulsant." AddGene. http://www.addgene.org/search/advanced/?q=190241. Deposited 3 August 2022.